

Local stiffness matrices for the semi-analytical Finite Strip Method in case of various boundary conditions

Dávid Visy / Sándor Ádány

Received 2014-02-07, revised 2014-05-21, accepted 2014-05-29

Abstract

In this paper the elastic and geometric stiffness matrices of the semi-analytical finite strip method (FSM) are discussed. The stiffness matrices are derived in various options. New derivations are presented for different longitudinal base functions, which corresponds to column/beam member with general boundary conditions. Numerical studies are performed to verify the new stiffness matrices as well as to illustrate the effect of the various options. It is shown that inconsistency is existing in the current implementations of FSM, which inconsistency has negligible effect in most of the practical cases, but might have non-negligible effect in certain specific cases.

Keywords

semi-analytical Finite Strip Method · elastic and geometric stiffness matrices

1 Introduction

Buckling has crucial role in the behaviour of thin-walled members. It is buckling which makes the behaviour and design of a thin-walled member far more complex than those of typical compact sections used in structural engineering. Since the load carrying capacity of thin-walled members is often governed by buckling phenomena, the ability to calculate the associated elastic critical loads is of great importance. In current design codes, e.g. relevant Eurocode [14], the accurate calculation of the elastic critical loads is crucial in predicting the ultimate load carrying capacity of a thin-walled member.

Analytical formulae exist for the calculation of certain buckling loads, but their applicability is limited. Therefore, numerical methods are widely used, including e.g., the shell Finite Element Method (FEM), or the (constrained) Finite Strip Method (FSM or cFSM). FEM is certainly the most well-known and most general, but FSM is also popular since it is much faster and easier to use than FEM. The presented research focuses on the FSM, more exactly on the FSM version with no longitudinal discretization, as proposed by Cheung [9], than applied by Schafer in the CUFSM software ([15] and [10]). Recently a special version of FSM has been proposed, called constrained Finite Strip Method (cFSM), presented in [4]. cFSM uses mechanical criteria to enforce or classify deformations to be consistent with global (G), distortional (D), local (L), and other (i.e., shear and transverse extension, S+T) deformations. cFSM is implemented in CUFSM, too. Both FSM and cFSM are widely used in the analysis of thin-walled members. FSM is the essential part of the Direct Strength Method which is developed to predict the load bearing capacity of thin-walled cold-formed steel members, which now is included in the relevant North-American design code [18]. FSM/cFSM is also widely applied in recent researches, e.g. in searching for optimized shape of cold-formed steel members' cross-sections ([7] and [6]), in characterizing the geometrical imperfections of cold-formed steel members [8], or in identifying deformations of thin-walled columns or beams calculated by shell FEM analysis [5].

Recent analytical studies (see [1] and [2]) showed some inconsistency in CUFSM caused by the inconsistent handling

Dávid Visy

Department of Structural Mechanics, Budapest University of Technology and Economics, Műegyetem rkp. 3, H-1111 Budapest, Hungary
e-mail: davidvisy@mail.bme.hu

Sándor Ádány

Department of Structural Engineering, Budapest University of Technology and Economics, Műegyetem rkp. 3, H-1111 Budapest, Hungary
e-mail: sadany@epito.bme.hu

of through-thickness variation of strains-stresses. In recent CUFSM the through-thickness variation is neglected in the work of the external forces (i.e. the negative of the external potential energy), while in the internal strain energy (i.e. in the internal potential energy) the through-thickness variation is considered. The practical effect of the inconsistency was discussed in the frame of global buckling (e.g., flexural, torsional, lateral-torsional buckling), and was concluded that the inconsistency has practically negligible effect on the vast majority of practical cases, but examples are found when this inconsistency has non-negligible effect, e.g. in case of short members, thicker cross-sections, and especially for torsional type buckling modes (i.e. pure-torsional, flexural-torsional and lateral-torsional buckling).

As the inconsistency comes from the different assumptions of internal and external potential energy, the problem is embedded in the derivation of elastic and geometric stiffness matrices. In a recent paper [11] the derivations are presented for the simplest case: members with (globally and locally) pinned ends. However, in the latest version of CUFSM software, Li and Schafer introduced the solution for general boundary conditions [13].

In this paper the derivation of stiffness matrices is generalized in two ways: (i) various longitudinal base functions are considered as in [3] and [13] (which correspond to various end restraints: simple-simple, clamped-clamped, simple-clamped, clamped-free and clamped-guided), and (ii) a general distribution of the loads is assumed over the strip. As in [11] the elastic stiffness matrix is derived in two different versions: through-thickness variation is considered or neglected in the internal strain energy. The geometric stiffness matrix is derived in four different ways: through-thickness variation is considered or neglected in the work of the external forces, and the second-order term of the longitudinal displacement is considered or neglected in the second-order strain. The different stiffness matrices are derived in closed form with these assumptions, and implemented into the recent version of CUFSM software. With the modified software numerical studies are performed to verify the new stiffness matrices as well as to illustrate the effect of the various options. Critical stresses are calculated for general buckling cases, and also for pure buckling modes: global (i.e. flexural, torsional, lateral-torsional), distortional and local plate buckling. These FSM critical values are compared to each other and to Shell FEM, Beam FEM and generalized beam theory (GBT) results.

2 Finite strip method stiffness matrices

2.1 Overview of the derivations

In the semi-analytical finite strip method a member is discretized into longitudinal strips, unlike in finite element method which applies discretization in both the longitudinal and transverse directions. In Fig. 1 a single strip is highlighted, along with the local coordinate system and the degrees of freedom (DOF) for the strip, the dimensions of the strip, and the applied end tractions. Unlike in previous FSM derivations (see [10]), here the dependency of the displacements on the local z coordi-

nate is explicitly considered, otherwise the usual steps of finite element or finite strip derivations are followed. It is to highlight that here the positive sign of the rotational degree of freedom, Θ , corresponds to the positive rotation in the coordinate system, which is just the opposite the sign convention used in [9], [13] and [10].

$$T = T_{y0} + T'_x x + T'_{z1} z + \frac{T'_{z2} - T'_{z1}}{b} xz \quad (1)$$

where T_{y0} is the load on one end of the mid-line at $x = 0$ point, T'_x is the variation in x direction, while T'_{z1} and T'_{z2} are the variations in z direction at $x = 0$ and $x = b$ points.

The vector of general displacement field, \mathbf{u} , is approximated with the matrix of shape functions, $\mathbf{N}_{[m]}$, and the vector of the nodal line displacements, $\mathbf{d}_{[m]}$, as:

$$\mathbf{u} = \begin{bmatrix} u(x, y, z) \\ v(x, y, z) \\ w(x, y, z) \end{bmatrix} = \sum_{m=1}^q \mathbf{N}_{[m]} \mathbf{d}_{[m]} \quad (2)$$

where

$$\mathbf{N}_{[m]} = \begin{bmatrix} \mathbf{N}_{\mathbf{u}[m]} & -z \frac{\partial \mathbf{N}_{\mathbf{w}[m]}}{\partial x} \\ \mathbf{N}_{\mathbf{v}[m]} & -z \frac{\partial \mathbf{N}_{\mathbf{w}[m]}}{\partial y} \\ \mathbf{0} & \mathbf{N}_{\mathbf{w}[m]} \end{bmatrix} \quad (3)$$

and

$$\mathbf{d}_{[m]} = \begin{bmatrix} u_{1[m]} & v_{1[m]} & u_{2[m]} & v_{2[m]} \\ w_{1[m]} & \Theta_{1[m]} & w_{2[m]} & \Theta_{2[m]} \end{bmatrix}^T \quad (4)$$

The shape functions for approximation of in-plane displacements from u and v are $\mathbf{N}_{\mathbf{u}[m]}$ and $\mathbf{N}_{\mathbf{v}[m]}$, while the shape function for approximation of out-of-plane displacement from w and Θ is $\mathbf{N}_{\mathbf{w}[m]}$, as:

$$\mathbf{N}_{\mathbf{u}[m]} = \begin{bmatrix} \left(1 - \frac{x}{b}\right) & 0 & \left(\frac{x}{b}\right) & 0 \end{bmatrix} Y_{[m]} \quad (5)$$

$$\mathbf{N}_{\mathbf{v}[m]} = \begin{bmatrix} 0 & \left(1 - \frac{x}{b}\right) & 0 & \left(\frac{x}{b}\right) \end{bmatrix} Y'_{[m]} \frac{1}{c_{[m]}} \quad (6)$$

$$\mathbf{N}_{\mathbf{w}[m]} = \begin{bmatrix} \left(1 - \frac{3x^2}{b^2} + \frac{2x^3}{b^3}\right) & -\left(x - \frac{2x^2}{b} + \frac{x^3}{b^2}\right) \\ \left(\frac{3x^2}{b^2} - \frac{2x^3}{b^3}\right) & -\left(-\frac{x^2}{b} + \frac{x^3}{b^2}\right) \end{bmatrix} Y_{[m]} \quad (7)$$

The approximation in the transverse directions is the same as a classical beam finite element (using the Hermite polynomials), while in the longitudinal direction $Y_{[m]}$ is applied, which is a trigonometric function depending on the end boundary conditions (see [3]). In $\mathbf{N}_{\mathbf{v}[m]}$ the parameter $c_{[m]} = m\pi/a$. For different end boundary conditions, the $Y_{[m]}$ functions are the following:

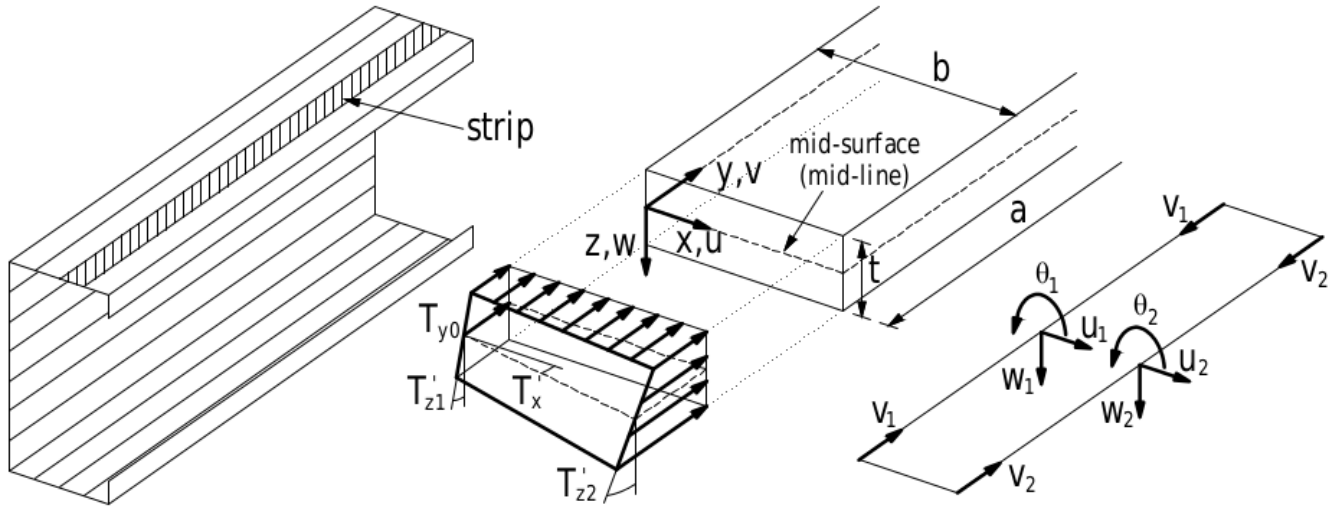


Fig. 1. Coordinate system, degrees of freedom and loads of a strip

S-S: simple-simple

$$Y_{[m]} = \sin \frac{m\pi y}{a} \quad (8)$$

C-C: clamped-clamped

$$Y_{[m]} = \sin \frac{m\pi y}{a} \sin \frac{\pi y}{a} \quad (9)$$

S-C: simple-clamped

$$Y_{[m]} = \sin \frac{(m+1)\pi y}{a} + \left(m + \frac{1}{m}\right) \sin \frac{m\pi y}{a} \quad (10)$$

C-F: clamped-free

$$Y_{[m]} = 1 - \cos \frac{(m-1/2)\pi y}{a} \quad (11)$$

C-G: clamped-guided

$$Y_{[m]} = \sin \frac{(m-1/2)\pi y}{a} \sin \frac{\pi y}{2a} \quad (12)$$

It is to mention that later $c_{[n]}$, Y_n , $\mathbf{N}_{u[n]}$, etc. symbols will also be used, see e.g., Eq. (32) or Eq. (38), with $c_{[n]} = n\pi/a$, $Y_{[n]} = \sin \frac{n\pi y}{a}$, etc.

The strain vector, ϵ , can be expressed by the operator matrix, \mathbf{L} , the matrix of shape functions, $\mathbf{N}_{[m]}$ (see Eq. (3)), and the vector of the nodal line displacements, $\mathbf{d}_{[m]}$ (see Eq. (4)), as:

$$\epsilon = \begin{bmatrix} \epsilon_x(x, y, z) \\ \epsilon_y(x, y, z) \\ \gamma_{xy}(x, y, z) \end{bmatrix} = \sum_{m=1}^q \mathbf{B}_{[m]} \mathbf{d}_{[m]} = \mathbf{L} \sum_{m=1}^q \mathbf{N}_{[m]} \mathbf{d}_{[m]} \quad (13)$$

where the operator matrix is:

$$\mathbf{L} = \begin{bmatrix} \frac{\partial}{\partial x} & 0 & 0 \\ 0 & \frac{\partial}{\partial y} & 0 \\ \frac{\partial}{\partial y} & \frac{\partial}{\partial x} & 0 \end{bmatrix} \quad (14)$$

The stress vector, σ , can be expressed with the material matrix, \mathbf{E} , and the strain vector, ϵ , as:

$$\sigma = \mathbf{E}\epsilon, \quad (15)$$

where the material matrix, assuming linear elastic orthotropic material, is:

$$\mathbf{E} = \begin{bmatrix} E_{11} & E_{12} & 0 \\ E_{21} & E_{22} & 0 \\ 0 & 0 & G \end{bmatrix} = \begin{bmatrix} \frac{E_x}{1-\nu_{xy}\nu_{yx}} & \frac{\nu_{yx}E_x}{1-\nu_{xy}\nu_{yx}} & 0 \\ \frac{\nu_{xy}E_y}{1-\nu_{xy}\nu_{yx}} & \frac{E_y}{1-\nu_{xy}\nu_{yx}} & 0 \\ 0 & 0 & G \end{bmatrix} \quad (16)$$

and the stress vector is:

$$\sigma = \begin{bmatrix} \sigma_x(x, y, z) \\ \sigma_y(x, y, z) \\ \tau_{xy}(x, y, z) \end{bmatrix} \quad (17)$$

Since the method is intended to be applicable for geometrically nonlinear analysis (e.g., linear buckling analysis), nonlinear strains must be considered. This is completed here by using the second-order terms of Green-Lagrange strains. However, since longitudinal loading is assumed only, it is the longitudinal normal strain only where second-order term is necessary (similarly to [9],[13] and [10]), as follows:

$$\epsilon_y^H = \frac{1}{2} \left[\left(\frac{\partial u}{\partial y} \right)^2 + \left(\frac{\partial v}{\partial y} \right)^2 + \left(\frac{\partial w}{\partial y} \right)^2 \right] \quad (18)$$

which can be expressed with the matrix of shape functions and the vector of the nodal line displacements using Eqs. (3) and (4), as:

$$\begin{aligned} \epsilon_y^H &= \frac{1}{2} \sum_{m=1}^q \sum_{n=1}^q \mathbf{d}_{[m]}^T \frac{\partial \mathbf{N}_{[m]}^T}{\partial y} \frac{\partial \mathbf{N}_{[n]}}{\partial y} \mathbf{d}_{[n]} = \\ &= \frac{1}{2} \sum_{m=1}^q \sum_{n=1}^q \mathbf{d}_{[m]}^T \mathbf{G}_{[m]}^T \mathbf{G}_{[n]} \mathbf{d}_{[n]} \end{aligned} \quad (19)$$

The total potential energy, Π , can be calculated from the internal strain energy, U , and the work of the external forces, W , (i.e., the negative of the external potential), as:

$$\Pi = U - W \quad (20)$$

The internal strain energy, U , can be expressed using Eqs. (13) and (15), as:

$$\begin{aligned} U &= \frac{1}{2} \int_V \boldsymbol{\sigma}^T \boldsymbol{\epsilon} dV = \frac{1}{2} \int_V \boldsymbol{\epsilon}^T \mathbf{E} \boldsymbol{\epsilon} dV = \\ &= \frac{1}{2} \sum_{m=1}^q \sum_{n=1}^q \mathbf{d}_{[m]}^T \left[\int_V \mathbf{B}_{[m]}^T \mathbf{E} \mathbf{B}_{[n]} dV \right] \mathbf{d}_{[n]} = \\ &= \frac{1}{2} \sum_{m=1}^q \sum_{n=1}^q \mathbf{d}_{[m]}^T \mathbf{k}_{e[mn]} \mathbf{d}_{[n]} \end{aligned} \quad (21)$$

The work of the external forces, W , can be written as follows, using Eqs. (1) and (19):

$$\begin{aligned} W &= \int_V T \epsilon_y^I dV = \\ &= \frac{1}{2} \sum_{m=1}^q \sum_{n=1}^q \mathbf{d}_{[m]}^T \left[\int_V T \mathbf{G}_{[m]}^T \mathbf{G}_{[n]} dV \right] \mathbf{d}_{[n]} = \\ &= \frac{1}{2} \sum_{m=1}^q \sum_{n=1}^q \mathbf{d}_{[m]}^T \mathbf{k}_{g[mn]} \mathbf{d}_{[n]} \end{aligned} \quad (22)$$

In Eq. (21) the elastic stiffness matrix, while in Eq. (22) the geometric stiffness matrix appears, as a function of the m and n parameters:

$$\mathbf{k}_{e[mn]} = \int_V \mathbf{B}_{[m]}^T \mathbf{E} \mathbf{B}_{[n]} dV \quad (23)$$

$$\mathbf{k}_{g[mn]} = \int_V T \mathbf{G}_{[m]}^T \mathbf{G}_{[n]} dV \quad (24)$$

2.2 The different options

Though the above steps of the derivation are always valid, simplifications in the formulae are possible and sometimes applied. Simplification is possible at three steps, namely: (i) definition of second-order strain, (ii) integration in the work of the external forces, and (iii) integration in internal strain energy. These possible simplifications are shown as follows.

In classical finite strip derivations (see [9] and [10]) as well as in finite element derivations the second-order strain term is expressed as shown in Eq. (18). However, it is also common to use a simplified formula, too, with neglecting the second-order term of the longitudinal displacement (i.e., neglecting the $(\partial v / \partial y)^2$ term). This simplified formula is the one typically used in classical buckling solutions of beams and columns. Therefore, the second-order strain term will be considered here in two options, as:

$$\epsilon_y^I = \frac{1}{2} \left[\left(\frac{\partial u}{\partial y} \right)^2 + \left(\frac{\partial v}{\partial y} \right)^2 + \left(\frac{\partial w}{\partial y} \right)^2 \right] \quad (25)$$

$$\epsilon_y^I = \frac{1}{2} \left[\left(\frac{\partial u}{\partial y} \right)^2 + \left(\frac{\partial w}{\partial y} \right)^2 \right] \quad (26)$$

Furthermore, in performing the integration to calculate the work of the external forces (see Eq. (22)), two options are used in the practice, as follows:

$$W = \int_{-t/2}^{t/2} \int_0^a \int_0^b T \epsilon_y^I dx dy dz \quad (27)$$

$$W = t \int_0^a \int_0^b T \epsilon_y^I dx dy \quad (28)$$

The formula in Eq. (27) is the mathematically precise one, but the other formula (in Eq. (28)) is also widely used, especially in case of thin-walled members where the effect of the variation through the thickness is considered to be negligible. (Note, in case of the formula in Eq. (28), both T and ϵ_y^I functions should be considered with their mean values, i.e. with substituting $z = 0$.)

Finally, in calculating the internal strain energy (see Eq. (21)), two options might be established (similarly to those of the external work), as:

$$U = \frac{1}{2} \int_{-t/2}^{t/2} \int_0^a \int_0^b \boldsymbol{\sigma}^T \boldsymbol{\epsilon} dx dy dz \quad (29)$$

$$U = \frac{1}{2} t \int_0^a \int_0^b \boldsymbol{\sigma}^T \boldsymbol{\epsilon} dx dy \quad (30)$$

The variation of strains and stresses through the thickness can be considered (see Eq. (29)) or disregarded (see Eq. (30)), which latter case corresponds to neglecting the bending energy. (Again, in case of the formula in Eq. (30), both $\boldsymbol{\sigma}^T$ and $\boldsymbol{\epsilon}$ functions should be considered with their mean values, i.e. with substituting $z = 0$.)

Thus, there are altogether eight different versions, as summarized in Tab. 1. As far as the options are concerned, here are some remarks:

- The first two options have influence on the geometric stiffness matrix, but no influence on the elastic stiffness matrix. On the other hand, the third option has influence on the elastic stiffness matrix only. This means that the elastic stiffness matrix (\mathbf{k}_e) can be defined in two versions, while the geometric stiffness matrix (\mathbf{k}_g) in four versions.
- The classical FSM (see [9] and [10]) uses *yny* version.
- It does not seem to be consistent to consider through-thickness variation at one step of the derivation, while disregard it in another step, thus, **ny* or **yn* versions are theoretically inconsistent (even though this inconsistency might have negligibly small practical effect).
- If a version is referenced with *** in it, that means it can be both yes or no (e.g. **ny* summarizes the *nyy* and *yny* versions).

2.3 Different versions of the elastic stiffness matrix

The elastic stiffness matrix appears in the calculation of internal strain energy (see Eq. (21)). As it mentioned in Section 2.2, there are two different ways for the calculation of the internal potential: the through-thickness stress-strain variation can be

Tab. 1. Definition of the different calculation versions according to the three options

Options	Different versions							
	<i>nnn</i>	<i>nny</i>	<i>nyn</i>	<i>nyy</i>	<i>ynn</i>	<i>yny</i>	<i>yyn</i>	<i>yyy</i>
$(\partial v/\partial y)^2$ term considered?	No	No	No	No	Yes	Yes	Yes	Yes
Through-thickness integration in external work W ?	No	No	Yes	Yes	No	No	Yes	Yes
Through-thickness integration in internal potential U ?	No	Yes	No	Yes	No	Yes	No	Yes

considered (as in Eq. (29)), or can be neglected (as in Eq. (30)). It also means that the elastic stiffness matrix has two different versions, one is the $\mathbf{k}_{e[mn]}^{**n}$ matrix in case of neglect, the other is the $\mathbf{k}_{e[mn]}^{**y}$ matrix, when through-thickness stress-strain variation is considered. The substitution and subsequent integration leads to the following closed-form solution for the $**n$ version:

$$\mathbf{k}_{e[mn]}^{**n} = \begin{bmatrix} \mathbf{k}_{e,11[mn]}^{**n} & \mathbf{0} \\ \mathbf{0} & \mathbf{0} \end{bmatrix} \quad (31)$$

where $\mathbf{0}$ denotes a four-by-four zero matrix, and the non-zero term is expressed as:

$$\mathbf{k}_{e,11[mn]}^{**n} = t \begin{bmatrix} \frac{3E_{11}I_1 + Gb^2I_5}{3b} & -\frac{E_{12}I_3 + GI_5}{2c_{[m]}} & -\frac{6E_{11}I_1 + Gb^2I_5}{6b} & -\frac{E_{12}I_3 + GI_5}{2c_{[m]}} \\ -\frac{E_{21}I_2 + GI_5}{2c_{[m]}} & \frac{E_{22}b^2I_4 + 3GI_5}{3bc_{[m]}c_{[n]}} & \frac{E_{21}I_2 - GI_5}{2c_{[m]}} & \frac{E_{22}b^2I_4 - 6GI_5}{6bc_{[m]}c_{[n]}} \\ -\frac{6E_{11}I_1 + Gb^2I_5}{6b} & \frac{E_{12}I_3 - GI_5}{2c_{[m]}} & \frac{3E_{11}I_1 + Gb^2I_5}{2c_{[m]}} & \frac{E_{12}I_3 + GI_5}{2c_{[m]}} \\ -\frac{E_{21}I_2 + GI_5}{2c_{[m]}} & \frac{E_{22}b^2I_4 - 6GI_5}{6bc_{[m]}c_{[n]}} & \frac{E_{21}I_2 + GI_5}{2c_{[m]}} & \frac{E_{22}b^2I_4 + 3GI_5}{3bc_{[m]}c_{[n]}} \end{bmatrix} \quad (32)$$

In case of $**y$ version, the elastic stiffness matrix can be calculated from the $**n$ version (see Eq. (31)) with an additional matrix, $\Delta\mathbf{k}_{e[mn]}^{**y}$, as:

$$\mathbf{k}_{e[mn]}^{**y} = \mathbf{k}_{e[mn]}^{**n} + \Delta\mathbf{k}_{e[mn]}^{**y} \quad (33)$$

where

$$\Delta\mathbf{k}_{e[mn]}^{**y} = \begin{bmatrix} \mathbf{0} & \mathbf{0} & \mathbf{0} \\ \mathbf{0} & \Delta\mathbf{k}_{e,22[mn]}^{**y} & \Delta\mathbf{k}_{e,23[mn]}^{**y} \\ \mathbf{0} & \Delta\mathbf{k}_{e,32[mn]}^{**y} & \Delta\mathbf{k}_{e,33[mn]}^{**y} \end{bmatrix} \quad (34)$$

and the two-by-two submatrices are:

$$\Delta\mathbf{k}_{e,22[mn]}^{**y} = t^3 \begin{bmatrix} \left(\frac{E_{11}I_1}{b^3} - \frac{E_{12}I_3 + E_{21}I_2}{10b} \right) & \left(-\frac{E_{11}I_1}{2b^2} + \frac{E_{12}I_3 + 11E_{21}I_2}{120} \right) \\ \left(+\frac{13E_{22}bI_4}{420} + \frac{2GI_5}{5b} \right) & \left(-\frac{11E_{22}b^2I_4}{2520} - \frac{GI_5}{30} \right) \\ \left(-\frac{E_{11}I_1}{2b^2} + \frac{11E_{12}I_3 + E_{21}I_2}{120} \right) & \left(\frac{E_{11}I_1}{3b} - \frac{E_{12}bI_3 + E_{21}bI_2}{90} \right) \\ \left(-\frac{11E_{22}b^2I_4}{2520} - \frac{GI_5}{30} \right) & \left(+\frac{E_{22}b^3I_4}{1260} + \frac{2Gbl_5}{45} \right) \end{bmatrix} \quad (35)$$

$$\Delta\mathbf{k}_{e,23[mn]}^{**y} = \Delta\mathbf{k}_{e,32[mn]}^{**y} = t^3 \begin{bmatrix} \left(-\frac{E_{11}I_1}{b^3} + \frac{E_{12}I_3 + E_{21}I_2}{10b} \right) & \left(-\frac{E_{11}I_1}{2b^2} + \frac{E_{12}I_3 + E_{21}I_2}{120} \right) \\ \left(+\frac{3E_{22}bI_4}{280} - \frac{2GI_5}{5b} \right) & \left(+\frac{13E_{22}b^2I_4}{5040} - \frac{GI_5}{30} \right) \\ \left(\frac{E_{11}I_1}{2b^2} - \frac{E_{12}I_3 + E_{21}I_2}{120} \right) & \left(\frac{E_{11}I_1}{6b} + \frac{E_{12}bI_3 + E_{21}bI_2}{360} \right) \\ \left(-\frac{13E_{22}b^2I_4}{5040} + \frac{GI_5}{30} \right) & \left(-\frac{E_{22}b^3I_4}{1680} - \frac{Gbl_5}{90} \right) \end{bmatrix} \quad (36)$$

$$\Delta\mathbf{k}_{e,33[mn]}^{**y} = t^3 \begin{bmatrix} \left(\frac{E_{11}I_1}{b^3} - \frac{E_{12}I_3 + E_{21}I_2}{10b} \right) & \left(\frac{E_{11}I_1}{2b^2} - \frac{E_{12}I_3 + 11E_{21}I_2}{120} \right) \\ \left(+\frac{13E_{22}bI_4}{420} + \frac{2GI_5}{5b} \right) & \left(-\frac{11E_{22}b^2I_4}{2520} + \frac{GI_5}{30} \right) \\ \left(\frac{E_{11}I_1}{2b^2} - \frac{11E_{12}I_3 + E_{21}I_2}{120} \right) & \left(\frac{E_{11}I_1}{3b} - \frac{E_{12}bI_3 + E_{21}bI_2}{90} \right) \\ \left(+\frac{11E_{22}b^2I_4}{2520} + \frac{GI_5}{30} \right) & \left(+\frac{E_{22}b^3I_4}{1260} + \frac{2Gbl_5}{45} \right) \end{bmatrix} \quad (37)$$

The parameters in the matrices are $c_{[m]} = m\pi/a$, $c_{[n]} = n\pi/a$, and:

$$\begin{aligned} I_1 &= \int_0^a Y_{[m]}Y_{[n]}dy & I_2 &= \int_0^a Y'_{[m]}Y_{[n]}dy \\ I_3 &= \int_0^a Y_{[m]}Y''_{[n]}dy & I_4 &= \int_0^a Y'_{[m]}Y'_{[n]}dy \\ I_5 &= \int_0^a Y'_{[m]}Y'_{[n]}dy \end{aligned} \quad (38)$$

where I_1 - I_5 parameters have explicit integration results for all the five end boundary conditions (see Eqs. (8)-(12)), discussed in paper [13].

2.4 Different versions of the geometric stiffness matrix

The geometric stiffness matrix appears in the calculation of the work of external loads (see Eq. (22)). As it discussed in Section 2.2, there are four different ways for the calculation of the external work: in the second-order strain the $(\partial v/\partial y)^2$ term can be considered (as in Eq. (25)) or neglected (see Eq. (26)), while in the calculation of external work, the through-thickness variation can be considered (as in Eq. (27)), or neglected (see Eq. (28)), too. It means that the geometric stiffness matrix has altogether four different versions.

The simplest option is the nn^* version. In this case, the $\mathbf{k}_{g[mn]}^{nn^*}$ matrix can be written as:

$$\mathbf{k}_{g[mn]}^{nn^*} = \begin{bmatrix} \mathbf{k}_{g,11[mn]}^{nn^*} & \mathbf{0} \\ \mathbf{0} & \mathbf{k}_{g,22[mn]}^{nn^*} \end{bmatrix} \quad (39)$$

where the non-zero submatrices are:

$$\mathbf{k}_{g,11[mn]}^{nn^*} = btI_5 \begin{bmatrix} \frac{4T_{y0} + T_x b}{12} & 0 & \frac{2T_{y0} + T_x b}{12} & 0 \\ 0 & 0 & 0 & 0 \\ \frac{2T_{y0} + T_x b}{12} & 0 & \frac{4T_{y0} + 3T_x b}{12} & 0 \\ 0 & 0 & 0 & 0 \end{bmatrix} \quad (40)$$

and

$$\mathbf{k}_{g,22[mn]}^{nn*} = btI_5 \begin{bmatrix} \frac{13T_{y0}+3T_xb}{35} & \frac{22T_{y0}b+7T_xb^2}{420} & \frac{18T_{y0}+9T_xb}{140} & \frac{13T_{y0}b+6T_xb^2}{420} \\ \frac{22T_{y0}b+7T_xb^2}{420} & \frac{8T_{y0}b^2+3T_xb^3}{840} & \frac{13T_{y0}b+7T_xb^2}{420} & \frac{2T_{y0}b^2+T_xb^3}{280} \\ \frac{18T_{y0}+9T_xb}{140} & \frac{13T_{y0}b+7T_xb^2}{420} & \frac{13T_{y0}+10T_xb}{35} & \frac{22T_{y0}b+15T_xb^2}{420} \\ \frac{13T_{y0}b+6T_xb^2}{420} & \frac{2T_{y0}b^2+T_xb^3}{280} & \frac{22T_{y0}b+15T_xb^2}{420} & \frac{8T_{y0}b^2+5T_xb^3}{840} \end{bmatrix} \quad (41)$$

If the $(\partial v/\partial y)^2$ term is considered and the through-thickness variation is neglected, it leads to the yn^* version. The geometric stiffness matrix, $\mathbf{k}_{g[mn]}^{yn*}$, can be calculated using the nn^* version (see Eq. (39)) with an additional matrix, as:

$$\mathbf{k}_{g[mn]}^{yn*} = \mathbf{k}_{g[mn]}^{nn*} + \Delta\mathbf{k}_{g[mn]}^{yn*} \quad (42)$$

where

$$\Delta\mathbf{k}_{g[mn]}^{yn*} = \begin{bmatrix} \Delta\mathbf{k}_{g,11[mn]}^{yn*} & \mathbf{0} \\ \mathbf{0} & \mathbf{0} \end{bmatrix} \quad (43)$$

with

$$\Delta\mathbf{k}_{g,11[mn]}^{yn*} = btI_4 \begin{bmatrix} 0 & 0 & 0 & 0 \\ 0 & \frac{4T_{y0}+T_xb}{12c_{[m]}c_{[n]}} & 0 & \frac{2T_{y0}+T_xb}{12c_{[m]}c_{[n]}} \\ 0 & 0 & 0 & 0 \\ 0 & \frac{2T_{y0}+T_xb}{12c_{[m]}c_{[n]}} & 0 & \frac{4T_{y0}+3T_xb}{12c_{[m]}c_{[n]}} \end{bmatrix} \quad (44)$$

If the $(\partial v/\partial y)^2$ term is neglected and the through-thickness variation is considered, it leads to the ny^* version. The geometric stiffness matrix, $\mathbf{k}_{g[mn]}^{ny*}$, can be calculated in the same way as before, using the nn^* version (Eq. (39)) with an additional matrix, as:

$$\mathbf{k}_{g[mn]}^{ny*} = \mathbf{k}_{g[mn]}^{nn*} + \Delta\mathbf{k}_{g[mn]}^{ny*} \quad (45)$$

where

$$\Delta\mathbf{k}_{g[mn]}^{ny*} = \begin{bmatrix} \mathbf{0} & \Delta\mathbf{k}_{g,12[mn]}^{ny*} \\ \Delta\mathbf{k}_{g,21[mn]}^{ny*} & \Delta\mathbf{k}_{g,22[mn]}^{ny*} \end{bmatrix} \quad (46)$$

and the non-zero submatrices are

$$\Delta\mathbf{k}_{g,12[mn]}^{ny*} = \Delta\mathbf{k}_{g,21[mn]}^{ny*T} = t^3I_5 \begin{bmatrix} \frac{3T_{z1}+2T_{z2}}{120} & \frac{6T_{z1}b-T_{z2}b}{720} & \frac{3T_{z1}+2T_{z2}}{120} & \frac{4T_{z1}b+T_{z2}b}{720} \\ 0 & 0 & 0 & 0 \\ \frac{2T_{z1}+3T_{z2}}{120} & \frac{-T_{z1}b+4T_{z2}b}{720} & \frac{-2T_{z1}+3T_{z2}}{120} & \frac{-T_{z1}b+6T_{z2}b}{720} \\ 0 & 0 & 0 & 0 \end{bmatrix} \quad (47)$$

and

$$\Delta\mathbf{k}_{g,22[mn]}^{ny*} = t^3I_5 \begin{bmatrix} \frac{2T_{y0}+T_xb}{20b} & \frac{-T_{y0}+T_xb}{120} & \frac{-2T_{y0}+T_xb}{20b} & \frac{-T_{y0}}{120} \\ \frac{-T_{y0}+T_xb}{120} & \frac{4T_{y0}b+T_xb^2}{360} & \frac{T_{y0}+T_xb}{120} & \frac{-2T_{y0}b+T_xb^2}{720} \\ \frac{2T_{y0}+T_xb}{20b} & \frac{T_{y0}+T_xb}{360} & \frac{2T_{y0}+T_xb}{120} & \frac{T_{y0}}{720} \\ \frac{-T_{y0}}{120} & \frac{-2T_{y0}b+T_xb^2}{720} & \frac{T_{y0}}{120} & \frac{4T_{y0}b+3T_xb^2}{360} \end{bmatrix} \quad (48)$$

Finally, if both the $(\partial v/\partial y)^2$ term and the through-thickness variation are considered, it is resulted in the yy^* version. In this case the geometric stiffness matrix, $\mathbf{k}_{g[mn]}^{yy*}$, can be calculated summarizing the matrix of nn^* version (Eq. (39)), the additional matrices of yn^* and ny^* versions (Eqs. (43) and (46)), and an additional matrix, $\Delta\mathbf{k}_{g[mn]}^{yy*}$, as:

$$\mathbf{k}_{g[mn]}^{yy*} = \mathbf{k}_{g[mn]}^{nn*} + \Delta\mathbf{k}_{g[mn]}^{yn*} + \Delta\mathbf{k}_{g[mn]}^{ny*} + \Delta\mathbf{k}_{g[mn]}^{yy*} \quad (49)$$

where

$$\Delta\mathbf{k}_{g[mn]}^{yy*} = \begin{bmatrix} \mathbf{0} & \Delta\mathbf{k}_{g,12[mn]}^{yy*} \\ \Delta\mathbf{k}_{g,21[mn]}^{yy*} & \Delta\mathbf{k}_{g,22[mn]}^{yy*} \end{bmatrix} \quad (50)$$

and the non-zero submatrices are

$$\Delta\mathbf{k}_{g,12[mn]}^{yy*} = bt^3I_4 \begin{bmatrix} 0 & 0 & 0 & 0 \\ \frac{16T_{z1}+5T_{z2}}{720c_{[m]}} & \frac{2T_{z1}b+T_{z2}b}{720c_{[m]}} & \frac{-4T_{z1}+5T_{z2}}{720c_{[m]}} & \frac{-T_{z1}b+T_{z2}b}{720c_{[m]}} \\ 0 & 0 & 0 & 0 \\ \frac{-5T_{z1}+4T_{z2}}{720c_{[m]}} & \frac{T_{z1}b+T_{z2}b}{720c_{[m]}} & \frac{-5T_{z1}+16T_{z2}}{720c_{[m]}} & \frac{-T_{z1}b+2T_{z2}b}{720c_{[m]}} \end{bmatrix}, \quad (51)$$

$$\Delta\mathbf{k}_{g,21[mn]}^{yy*} = bt^3I_4 \begin{bmatrix} 0 & \frac{-16T_{z1}+5T_{z2}}{720c_{[n]}} & 0 & \frac{-5T_{z1}+4T_{z2}}{720c_{[n]}} \\ 0 & \frac{2T_{z1}b+T_{z2}b}{720c_{[n]}} & 0 & \frac{T_{z1}b+T_{z2}b}{720c_{[n]}} \\ 0 & \frac{-4T_{z1}+5T_{z2}}{720c_{[n]}} & 0 & \frac{-5T_{z1}+16T_{z2}}{720c_{[n]}} \\ 0 & \frac{-T_{z1}b+T_{z2}b}{720c_{[n]}} & 0 & \frac{-T_{z1}b+2T_{z2}b}{720c_{[n]}} \end{bmatrix} \quad (52)$$

and

$$\Delta\mathbf{k}_{g,22[mn]}^{yy*} = bt^3I_4 \begin{bmatrix} \frac{13T_{y0}+3T_xb}{420} & \frac{22T_{y0}b+7T_xb^2}{5040} & \frac{6T_{y0}+3T_xb}{560} & \frac{13T_{y0}b+6T_xb^2}{5040} \\ \frac{22T_{y0}b+7T_xb^2}{5040} & \frac{8T_{y0}b^2+3T_xb^3}{10080} & \frac{13T_{y0}b+7T_xb^2}{5040} & \frac{2T_{y0}b^2+T_xb^3}{3360} \\ \frac{6T_{y0}+3T_xb}{560} & \frac{13T_{y0}b+7T_xb^2}{10080} & \frac{13T_{y0}+10T_xb}{420} & \frac{22T_{y0}b+15T_xb^2}{5040} \\ \frac{13T_{y0}b+6T_xb^2}{5040} & \frac{2T_{y0}b^2+T_xb^3}{3360} & \frac{22T_{y0}b+15T_xb^2}{5040} & \frac{8T_{y0}b^2+5T_xb^3}{10080} \end{bmatrix} \quad (53)$$

The parameters in the matrices are $c_{[m]} = m\pi/a$, $c_{[n]} = n\pi/a$, while I_4 and I_5 are mentioned in Eq. (38).

2.5 Stiffness matrices of a member

The matrices derived in Section 2.3 and 2.4 are eight-by-eight submatrices of the full local elastic and geometric stiffness matrices of a single strip, \mathbf{k}_e and \mathbf{k}_g . Assuming $m = 1 \dots q$ and $n = 1 \dots q$, both matrices can be expressed from q^2 submatrices, as follows:

$$\mathbf{k}_e = \begin{bmatrix} \mathbf{k}_{e[11]} & \dots & \mathbf{k}_{e[1m]} & \dots & \mathbf{k}_{e[1n]} & \dots & \mathbf{k}_{e[1q]} \\ \vdots & \ddots & \vdots & \ddots & \vdots & \ddots & \vdots \\ \mathbf{k}_{e[m1]} & & \mathbf{k}_{e[mm]} & & \mathbf{k}_{e[mn]} & & \mathbf{k}_{e[mq]} \\ \vdots & & \vdots & \ddots & \vdots & & \vdots \\ \mathbf{k}_{e[n1]} & & \mathbf{k}_{e[nm]} & & \mathbf{k}_{e[nn]} & & \mathbf{k}_{e[nq]} \\ \vdots & & \vdots & & \vdots & \ddots & \vdots \\ \mathbf{k}_{e[q1]} & \dots & \mathbf{k}_{e[qm]} & \dots & \mathbf{k}_{e[qn]} & \dots & \mathbf{k}_{e[qq]} \end{bmatrix} \quad (54)$$

$$\mathbf{k}_g = \begin{bmatrix} \mathbf{k}_{g[11]} & \cdots & \mathbf{k}_{g[1m]} & \cdots & \mathbf{k}_{g[1n]} & \cdots & \mathbf{k}_{g[1q]} \\ \vdots & \ddots & & & & & \vdots \\ \mathbf{k}_{g[m1]} & & \mathbf{k}_{g[mm]} & & \mathbf{k}_{g[mn]} & & \mathbf{k}_{g[mq]} \\ \vdots & & & \ddots & & & \vdots \\ \mathbf{k}_{g[n1]} & & \mathbf{k}_{g[nm]} & & \mathbf{k}_{g[nn]} & & \mathbf{k}_{g[nq]} \\ \vdots & & & & & \ddots & \vdots \\ \mathbf{k}_{g[q1]} & \cdots & \mathbf{k}_{g[qm]} & \cdots & \mathbf{k}_{g[qn]} & \cdots & \mathbf{k}_{g[qq]} \end{bmatrix} \quad (55)$$

The global stiffness matrices of a member consists of multiple strips can be assembled using \mathbf{k}_e and \mathbf{k}_g . The matrices must be transformed at first from local to global coordinate system, then the global elastic and geometric stiffness matrices, \mathbf{K}_e and \mathbf{K}_g , can be compiled. Transformation of the stiffness matrices of strip j follows from:

$$\mathbf{K}_e^{(j)} = \mathbf{\Gamma}^{(j)T} \mathbf{k}_e^{(j)} \mathbf{\Gamma}^{(j)} \quad (56)$$

and

$$\mathbf{K}_g^{(j)} = \mathbf{\Gamma}^{(j)T} \mathbf{k}_g^{(j)} \mathbf{\Gamma}^{(j)} \quad (57)$$

where $\mathbf{\Gamma}^{(j)}$ is the 2D rotation matrix. The global stiffness matrices may be assembled as an appropriate summation of the local stiffness matrices for all the s strips:

$$\mathbf{K}_e = \sum_{\text{assembly}}^{j=1 \dots s} \mathbf{K}_e^{(j)} \quad (58)$$

and

$$\mathbf{K}_g = \sum_{\text{assembly}}^{j=1 \dots s} \mathbf{K}_g^{(j)} \quad (59)$$

3 Numerical studies

3.1 In general

The numerical studies are completed for two reasons: in order (i) to verify the newly derived stiffness matrices, and (ii) to show the effect of the different matrix options on the critical forces. The calculations are performed by a modified version of the CUFMS software [15], in which the new stiffness matrices are used. These results are compared to results of shell and beam finite element analysis by ANSYS [16], and to results of generalized beam theory by GBTUL [17].

Prismatic members are analyzed with a wide range of member lengths and various cross-sections: two I-sections, an I-section with two web-stiffeners and a C-section (see Fig. 2). Linearly elastic material is used with steel-like material constants: $E = 210000$ MPa, $G = 105000$ MPa, $\nu = 0$. It is to note that the Poisson's ratio is assumed to be zero for no other reason than to avoid the artificial stiffening effect of restrained (mid-plane) transverse extension which takes place in G and D modes for non-zero Poisson's ratios, as discussed in detail in [12]. Altogether five combination of end restraints are studied (but not all

of them appears in the results): simple-simple (S-S), clamped-clamped (C-C), simple-clamped (S-C), clamped-free (C-F) and clamped-guided (C-G) supports. In case of simple support the end is free to rotate about the transverse axes and free to warp, but restrained against transverse translations and rotation about the longitudinal axes. Clamped end is restrained against transverse translations, rotations about all axes and warping. Guided end is restrained against rotations about all axes and warping while free to move in the transverse directions (i.e., perpendicular to the member longitudinal axis). The members are loaded by two concentrated longitudinal forces (column with compression) or loaded by two concentrated moments (beam with bending) at both ends, equal in magnitude but opposite in direction, which results in a constant compression force or constant bending moment along the member.

In case of these members various buckling problems were studied, and elastic critical stresses were calculated. For a bended member the critical stresses are interpreted on the mid-line of the top/bottom flange. On the one hand general buckling modes were assumed: different interactions of global, distortional and local plate buckling. On the other hand the pure buckling modes were studied, including pure global modes (flexural, torsional and lateral-torsional buckling), pure local plate buckling and pure distortional buckling. In most of the cases only the first buckling modes were calculated, but for some instance the higher modes are shown, too.

3.2 Applied numerical models

The FSM results are compared to altogether three different numerical methods: shell and beam finite element methods by ANSYS, and generalized beam theory by GBTUL. Fig. 3 shows the main differences between the different methods.

In case of shell finite element model (Shell FEM) rectangular four-node shell elements are applied with six degrees of freedom on every node (three translational and three rotational), based on Kirchhoff plate theory (called SHELL63 in ANSYS). A relatively fine discretization is used with approx. 2000-20000 shell elements (depending on member length). The supports are applied in the gravity center of the end cross-section, and the other nodes of the cross-section are linked to this node with support-specific degrees of freedom: for simple support the transverse translational and the longitudinal rotational dofs, while for clamped and guided support all dofs are applied. This difference of the supports needs difference in the load application mode, too. In case of simple support (S) and free end (F) the forces or moments have been applied as linearly distributed loads on the lines of end cross-sections so that the resultant would be equal to a unit compression force or bending moment, while for clamped (C) and guided (G) supports the loads are applied on the nodes of the supports as a concentrated force or moment. To enforce the members to buckle according to desired modes the shell finite element model have to be constrained, which is not an obvious process, and depends on the desired

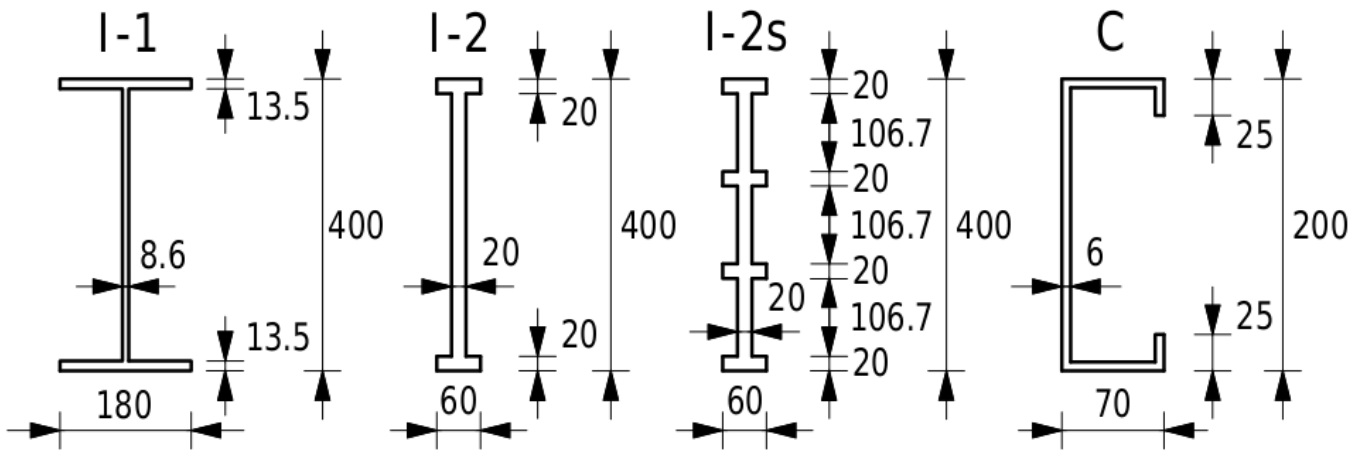


Fig. 2. The applied cross-sections

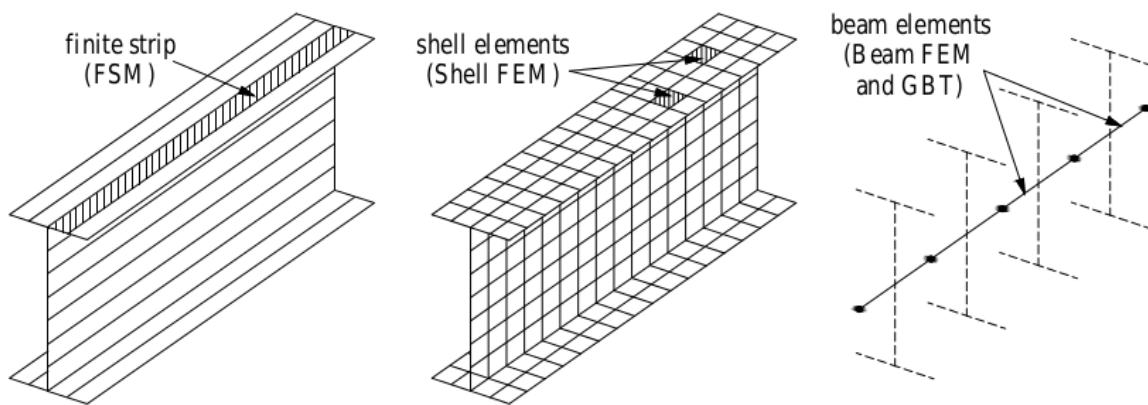


Fig. 3. The applied numerical models: FSM, Shell FEM, Beam FEM and GBT

buckling mode. For pure global buckling the constraining can be applied in three steps: (i) virtual diaphragms can be used for all cross-sections in order to exclude cross-section distortions, (ii) constraints can be applied in order to enforce linear warping distribution in transverse directions on each plate element, and (iii) shear panels can be used for each plate element in order to exclude the in-plane shear deformations. To enforce the member for pure local plate buckling only the shear panels are used out of above-mentioned constraints, and the corner points of the cross-sections are supported in both transverse directions. Finally, there is no simple way to enforce a general shell finite element model to buckle according to the pure distortional buckling mode, so distortional buckling is not studied by shell FEM.

For the beam finite element model (Beam FEM) three-node beam elements are used with seven degrees of freedom on every node (three translational, three rotational and warping), based on Timoschenko beam theory (called BEAM189 in ANSYS). A fine meshing is applied with approx. 10-100 beam elements (depending on member length). The supports and the loads have been applied on the member end nodes. In case of Beam FEM only the global, flexural buckling modes can be studied, as the cross-sections remains rigid with this beam element (even with the warping dof). To exclude the shear deformations, the shear modulus have been increased thousandfold.

Generalized beam theory (GBT) has also been used for comparison, with the GBTUL software [17]. With this method both the general (interacted) buckling modes and the pure buckling modes can be studied.

3.3 Results

In Fig. 4 critical stresses are presented, calculated from a standard FSM analysis with considering multiple m terms. Though the actual plot belongs to the C-section (Fig. 2) column member, the observed tendencies are generally valid for the majority of practical problems. It is to observe that only four options lead to buckling solutions, i.e., in a general FSM analysis the $**n$ options cannot be used. It is also to observe that the differences between the four valid options are rather small, and in fact negligible for a wide range of member lengths. Thus, the general conclusion is that any of $**y$ options lead to practically correct critical loads if the analyzed problem can be considered to be a 'standard' problem, i.e., standard thin-walled cross-section, standard loading, the length is not extremely small, there are no special constraints, etc. However, if the analyzed problem is less usual, the above general conclusions might not be always and exactly valid, which is also intended to be demonstrated here.

A special version of FSM has recently been proposed, called constrained Finite Strip Method (cFSM), presented in [4]. cFSM uses mechanical criteria to enforce or classify deformations to be consistent with global (G), distortional (D), local (L), and other (i.e., shear and transverse extension, S+T) deformations. Since cFSM is implemented in CUFSM, it is possible, and in fact, easy to perform the buckling analysis in a reduced displace-

ment field, and to have the critical loads specifically to global buckling (e.g., flexural buckling, torsional buckling, lateral-torsional buckling, etc), to distortional buckling or to local plate buckling. Since the enforced mechanical criteria can also be interpreted as special, unusual restraints, they are worth to investigate.

In Figs. 5-9 typical critical load vs. buckling length plots are presented for pure modes, namely: for flexural buckling of a column (Fig. 5), for pure torsional buckling of a column (Fig. 6), for lateral-torsional buckling of a beam (Fig. 7), for distortional buckling of column member (Fig. 8), and for local plate buckling of a column member (Fig. 9). The most important observations are as follows.

- Unlike in a general FSM buckling analysis, all the eight versions lead to reasonable results in case of global buckling. In case of distortional buckling, though all the eight versions can be solved, only the four $**y$ versions lead to reasonable critical loads (while the $**n$ versions lead to clearly wrong critical load values for longer buckling lengths). Finally, local buckling can be solved by using the four $**y$ versions, only.
- In case of global and distortional buckling, there is a distinct difference depending on how the longitudinal second-order strain term is assumed (Eq. (25) or (26)): critical loads of $n**$ versions go infinitely large as the member length tends to zero, while critical loads of $y**$ versions converge to a finite value as the member length tends to zero.
- When torsion is important in the global buckling, there is a distinct difference between $**n$ and $**y$ versions: $**n$ critical loads converge to zero, while $**y$ critical loads converge to a finite value as the member length tends to infinity.

Though the differences in between the various reasonable versions might be small, smaller differences still exist. These differences cannot be properly visualized in classical critical load vs. length plots, but can be examined numerically. In Tabs. 2-10 critical stress values are summarized, comparing the various versions to each other in various situations, and for a wide range of lengths. Tab. 2 shows results for a bended C-section beam in case of S-S support, considering multiple m terms, including all buckling mode possibilities. The last row of the table indicates the typical buckling modes. In Tabs. 3 and 4 the first seven buckling modes of a compressed C-section column and a bended I-2s section beam are summarized. And finally Tabs. 5-10 are showing results for pure buckling modes of different members: flexural buckling of a compressed I-1 section column with S-S support (Tab. 5) and the same buckling mode of a compressed I-2 section column with C-G support (Tab. 6) (it is to note, that GBT results are based on S-S support – which has the same buckling length as C-G support – by reason of GBTUL software limitation), torsional buckling of a compressed I-2 section column with C-C support (Tab. 7), lateral-torsional buckling of a bended I-2 section beam with S-S support (Tab. 8), distortional

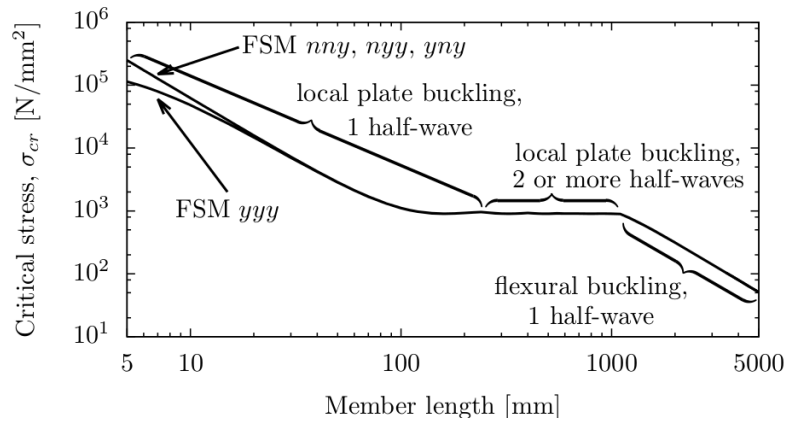


Fig. 4. Buckling of a compressed C-section column: tendencies

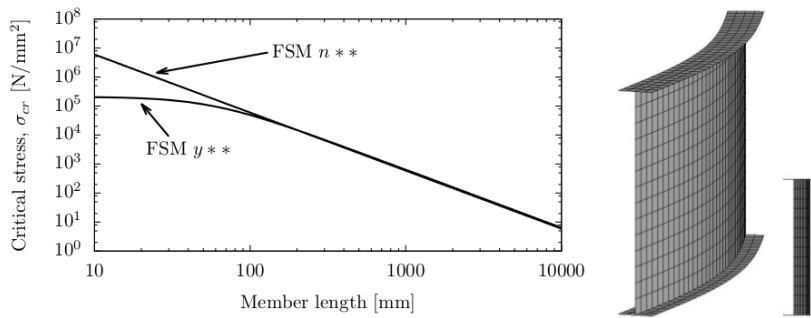


Fig. 5. Flexural buckling of a compressed I-section column: tendencies

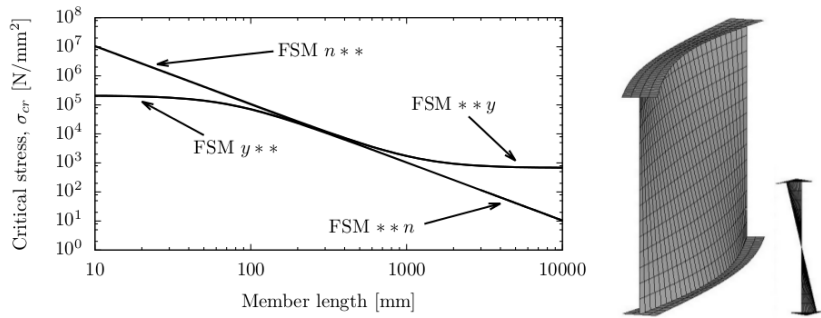


Fig. 6. Pure torsional buckling of a compressed I-section column: tendencies

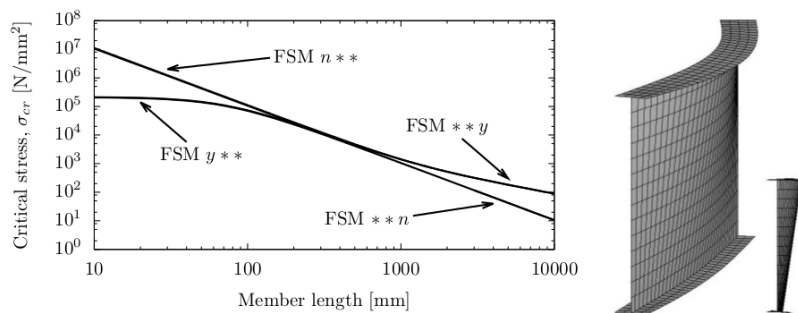


Fig. 7. Lateral-torsional buckling of a bended I-section beam: tendencies

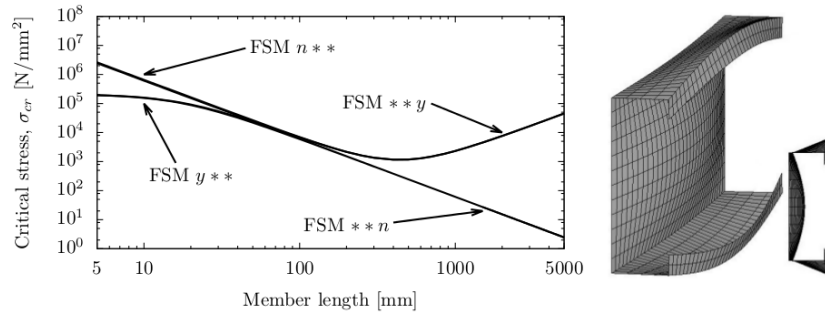


Fig. 8. Distortional buckling of a compressed C-section column: tendencies

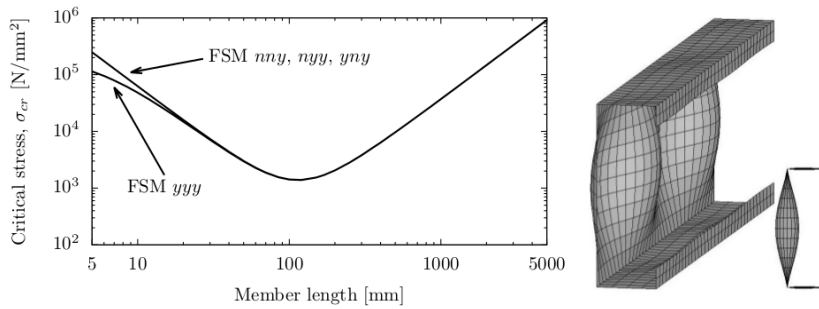


Fig. 9. Local plate buckling of a compressed C-section column: tendencies

Tab. 2. C-section beam, S-S support, all buckling mode possibilities

σ_{cr} [N/mm ²]	Length [mm]						
	5	10	50	100	500	1000	5000
FSM <i>nny</i>	252 381	65 840	7 031.7	4 727.7	2 324.8	1 936.4	152.93
FSM <i>nyy</i>	250 251	65 305	6 989.4	4 714.9	2 321.8	1 936.0	152.90
FSM <i>yny</i>	210 472	65 839	7 028.1	4 720.8	2 320.9	1 923.7	152.89
FSM <i>yyy</i>	115 080	50 477	6 904.6	4 694.4	2 317.8	1 923.2	152.86
Shell FEM	-	64 776	6 994.2	4 689.4	2 319.6	1 923.2	152.96
GBT	-	65 512	6 966.7	4 558.1	2 237.4	1 838.7	148.48
Buckling mode	L	L	L	L	D	G	G

Tab. 3. C-section column, L = 450 mm, C-C support, critical stress for the first seven modes

σ_{cr} [N/mm ²]	Buckling modes						
	1 st	2 nd	3 rd	4 th	5 th	6 th	7 th
FSM <i>nny</i>	1 002.3	1 026.7	1 315.4	1 387.2	1 785.1	1 939.9	2 432.5
FSM <i>nyy</i>	1 001.5	1 025.8	1 314.2	1 386.1	1 783.5	1 938.2	2 430.4
FSM <i>yny</i>	1 002.0	1 026.4	1 315.2	1 386.1	1 782.5	1 939.8	2 431.4
FSM <i>yyy</i>	999.5	1 024.0	1 309.8	1 380.7	1 774.4	1 924.7	2 408.1
Shell FEM	996.8	1 019.7	1 309.0	1 380.9	1 775.8	1 933.4	2 424.0
GBT	987.0	1 009.7	1 306.4	1 343.0	1 718.8	1 937.4	2 414.0
Buckling mode	L	L	L	D+L	D+L	L	D+L

Tab. 4. I-2s section beam, L = 500 mm, S-S support, critical stress for the first seven modes

σ_{cr} [N/mm ²]	Buckling modes						
	1 st	2 nd	3 rd	4 th	5 th	6 th	7 th
FSM <i>nny</i>	2 364,8	7 307,9	14 501	22 103	23 153	23 801	28 050
FSM <i>nyy</i>	2 362,2	7 300,2	14 484	21 990	22 761	23 399	27 687
FSM <i>yny</i>	2 350,4	7 135,4	13 849	20 970	23 025	23 309	27 005
FSM <i>yyy</i>	2 346,4	7 110,2	13 749	20 602	22 622	22 867	26 026
Shell FEM	2 351.5	7 139.9	13 853	20 941	23 030	23 321	26 886
Buckling mode	G	G	G	G+L	D	D	G+L

Tab. 5. I-1 section column, S-S support, critical stress for flexural buckling about minor axes

σ_{cr} [N/mm ²]	Length [mm]						
	10	50	100	500	1000	5000	10000
FSM <i>nnn</i>	3.323·10 ⁷	1 329 287	332 322	13 293	3 323.2	132.93	33.232
FSM <i>myy</i>	3.328·10 ⁷	1 331 362	332 841	13 314	3 328.4	133.14	33.284
FSM <i>nyn</i>	3.323·10 ⁷	1 329 287	332 322	13 293	3 323.2	132.93	33.232
FSM <i>nyy</i>	3.328·10 ⁷	1 331 362	332 841	13 314	3 328.4	133.14	33.284
FSM <i>yyn</i>	208 681	181 350	128 683	12 502	3 271.4	132.84	33.227
FSM <i>yny</i>	209 007	181 633	128 884	12 521	3 276.6	133.05	33.279
FSM <i>yyn</i>	208 358	181 106	128 560	12 500	3 271.4	132.84	33.227
FSM <i>yyy</i>	208 683	181 389	128 761	12 520	3 276.5	133.05	33.279
Shell FEM	209 043	181 648	128 812	12 521	3 276.7	133.18	33.292
Beam FEM	3.318·10 ⁷	1 329 719	332 738	13 312	3 328.3	133.14	33.285
GBT	3.328·10 ⁷	1 331 362	332 841	13 314	3 328.4	133.14	33.284

Tab. 6. I-2 section column, C-G support, critical stress for flexural buckling about minor axes

σ_{cr} [N/mm ²]	Length [mm]						
	10	50	100	500	1000	5000	10000
FSM <i>nnn</i>	1 492 284	59 691	14 923	596.91	149.23	5.9691	1.4923
FSM <i>myy</i>	2 017 347	80 694	20 173	806.94	201.73	8.0694	2.0173
FSM <i>nyn</i>	1 492 284	59 691	14 923	596.91	149.23	5.9691	1.4923
FSM <i>nyy</i>	2 017 347	80 694	20 173	806.94	201.73	8.0694	2.0173
FSM <i>yyn</i>	184 094	46 480	13 933	595.22	149.12	5.9690	1.4923
FSM <i>yny</i>	248 867	62 834	18 835	804.65	201.59	8.0692	2.0173
FSM <i>yyn</i>	140 696	43 122	13 615	594.63	149.09	5.9689	1.4923
FSM <i>yyy</i>	190 201	58 294	18 405	803.85	201.54	8.0691	2.0173
Shell FEM	-	62 842	18 834	804.70	201.59	8.0703	2.0189
Beam FEM	2 017 307	80 693	20 174	806.93	201.73	8.0694	2.0172
GBT (S-S supp.)	2 017 347	80 694	20 173	806.94	201.73	8.0694	2.0174

Tab. 7. I-2 section column, C-C support, critical stress for torsional buckling

σ_{cr} [N/mm ²]	Length [mm]						
	10	50	100	500	1000	5000	10000
FSM <i>nnn</i>	1.205·10 ⁷	482 035	120 509	4 820.4	1 205.1	48.20	12.05
FSM <i>myy</i>	1.348·10 ⁷	539 798	135 537	6 173.1	2 130.5	836.84	796.41
FSM <i>nyn</i>	1.203·10 ⁷	481 138	120 285	4 811.4	1 202.8	48.11	12.03
FSM <i>nyy</i>	1.345·10 ⁷	538 794	135 285	6 161.6	2 126.5	835.28	794.93
FSM <i>yyn</i>	206 403	146 275	76 569	4 712.2	1 198.2	48.19	12.05
FSM <i>yny</i>	230 815	163 803	86 118	6 034.6	2 118.3	836.65	796.37
FSM <i>yyn</i>	184 914	135 077	73 322	4 691.2	1 195.2	48.10	12.03
FSM <i>yyy</i>	206 784	151 263	82 466	6 007.7	2 113.0	835.07	794.88
Shell FEM	-	164 100	86 164	6 036.7	2 118.5	836.54	796.38
GBT	1.348·10 ⁷	539 798	135 537	6 173.1	2 130.5	836.84	796.41

Tab. 8. I-2 section beam, S-S support, critical stress for lateral-torsional buckling

σ_{cr} [N/mm ²]	Length [mm]						
	10	50	100	500	1000	5000	10000
FSM <i>nmn</i>	3 024 900	120 996	30 249	1 210.0	302.49	12.10	3.025
FSM <i>nny</i>	3 719 523	149 195	37 621	1 870.5	678.06	114.37	56.819
FSM <i>nyy</i>	3 023 542	120 942	30 235	1 209.4	302.35	12.09	3.024
FSM <i>nyy</i>	3 717 853	149 128	37 604	1 869.7	677.76	114.31	56.793
FSM <i>ynn</i>	196 367	76 766	26 440	1 203.0	302.05	12.10	3.025
FSM <i>yny</i>	241 460	94 657	32 884	1 859.8	677.09	114.36	56.818
FSM <i>yyy</i>	177 093	73 614	26 049	1 201.7	301.87	12.09	3.023
FSM <i>yyy</i>	217 760	90 770	32 397	1 857.7	676.67	114.31	56.792
Shell FEM	-	94 688	32 901	1 860.8	677.49	114.43	56.867
GBT	3 719 523	149 195	37 621	1 870.5	678.06	114.37	56.819

Tab. 9. I-2s section column, S-S support, critical stress for distortional buckling

σ_{cr} [N/mm ²]	Length [mm]						
	10	50	100	500	1000	5000	10000
FSM <i>nmn</i>	2 413 168	96 527	24 132	965.3	241.3	10	2
FSM <i>nny</i>	2 841 123	118 757	34 018	6 096.8	9 876.0	161 143	634 802
FSM <i>nyy</i>	2 383 612	95 344	23 836	953.4	238.4	10	2
FSM <i>nyy</i>	2 806 326	117 303	33 602	6 050.1	9 800.4	159 909	629 940
FSM <i>ynn</i>	193 188	66 130	21 644	960.9	241.0	10	2
FSM <i>yny</i>	221 916	81 360	30 512	6 064.3	9 862.8	161 135	634 793
FSM <i>yyy</i>	166 234	62 172	21 031	948.4	238.0	10	2
FSM <i>yyy</i>	195 714	76 491	29 647	6 013.8	9 785.6	159 900	629 931

Tab. 10. C-section column, S-S support, critical stress for local plate buckling

σ_{cr} [N/mm ²]	Length [mm]						
	5	10	50	100	500	1000	5000
FSM <i>nny</i>	249 061	62 528	2 878.3	1 119.2	3 632.1	13 294	323 032
FSM <i>nyy</i>	248 856	62 476	2 875.9	1 118.3	3 628.8	13 282	322 739
FSM <i>yny</i>	249 061	62 528	2 878.3	1 119.2	3 632.1	13 294	323 032
FSM <i>yyy</i>	113 978	48 213	2 842.3	1 115.0	3 628.4	13 281	322 739
Shell FEM	-	62 381	2 874.8	1 117.8	3 626.8	13 270	-
GBT	251 725	63 975	2 989.0	1 167.1	3 920.0	14 391	350 037

buckling of a compressed I-2s section column with S-S support (Tab. 9) and local plate buckling of a compressed C-section column with S-S support (Tab. 10). These tables are used also to compare the FSM results to results of other numerical methods, especially to shell finite element analysis and GBT analysis. The most important observations are as follows.

- In case of general cross-sections only small differences can be noticed (except in case of extremely small lengths).
- Shell FEM and FSM results are fairly similar. In case of global buckling, Shell FEM seems to be *yny* version. Coincidence of the Shell FEM and FSM results exists independently of end restraints or loading (i.e., compression or bending).
- Beam FEM results can be calculated just for global flexural buckling with the mentioned method. Beam FEM seems to be similar to FSM *yny* version.
- GBT and FSM results are similar, too. In case of global buckling GBT results practically exactly coincide with FSM *yny* version. In case of pure local buckling mode, GBTUL results are slightly different.
- If the cross-section is unusual, such as I-2, there are non-negligible differences between the versions, even in case of flexural buckling (see Tab. 6).
- In case of distortional buckling: the differences in between the reasonable ***y* versions are small, not more than 1% (see Tab. 9).
- In case of local buckling, the differences in between the valid (i.e., ***y*) versions is small, not more than a few percentage even if the plates are relatively thick (see Tab. 10).
- The differences are larger for higher buckling modes (see Tabs. 3 and 4).

It is also to note that various cFSM options are also compared to analytical results in case of global buckling, as summarized in [2], and excellent coincidence has been found.

4 Conclusions

In this paper elastic and geometric stiffness matrices for the semi-analytical finite strip method are derived. Altogether eight versions are considered and tested by numerical studies. The results justify the newly derived stiffness matrices as well as demonstrate the effect of various versions. Based on the results the general conclusions are as follows:

- In a general case ***y* versions can only be used, which means the through-thickness variation of the strains have to be considered, otherwise the calculation leads to false critical values.
- It is a question of decision how to consider the second-order (longitudinal) strain term (i.e. the $(\partial v/\partial y)^2$ term, as in Eq. (25) or (26)). Both alternatives are correct and widely used in practice, but lead to different results in case of short members.

- It seems to be more logical to use consistent versions (i.e., *nyy* or *yyy*), where the through-thickness variation of strains-stresses are both considered.
- Though *yny* version is theoretically inconsistent (as through-thickness variation is neglected in external work, but considered for the strains), it is found that *yny* version is widely used in practice, since shell FEM analysis - most probably - uses this version. In most cases the inaccuracy caused by the inconsistency of version *yny* is negligible.

Acknowledgement

The work reported in the paper has been developed in the framework of the project "Talent care and cultivation in the scientific workshops of BME". This project is supported by the grant TÁMOP-4.2.2.B-10/1-2010-0009. The work has also been financially supported by the OTKA K108912 project of the Hungarian Scientific Research Fund.

References

- 1 **Ádány S**, *Global buckling of thin-walled simply supported columns: Analytical solution based on shell model*, Thin-Walled Structures, **55**, (2012), 64–75, DOI 10.1016/j.tws.2012.02.002.
- 2 **Ádány S, Visy D**, *Global buckling of thin-walled simply supported columns: Numerical studies*, Thin-Walled Structures, **54**, (2012), 82–93, DOI 10.1016/j.tws.2012.02.001.
- 3 **Bradford MA, Azhari M**, *Buckling of plates with different end conditions using the finite strip method*, Computers & Structures, **56**(1), (1995), 75–83, DOI 10.1016/0045-7949(94)00528-B.
- 4 **Ádány S, Schafer BW**, *A full modal decomposition of thin-walled, single-branched open cross-section members via the constrained finite strip method*, Journal of Constructional Steel Research, **64**(1), (2008), 12–29, DOI 10.1016/j.jcsr.2007.04.004.
- 5 **Joó AL, Ádány S**, *FEM-based approach for the stability design of thin-walled members by using cFSM base functions*, Periodica Polytechnica Civil Engineering, **53**(2), (2009), 61–74, DOI 10.3311/pp.ci.2009-2.02.
- 6 **Leng J, Guest JK, Schafer BW**, *Shape optimization of cold-formed steel columns*, Thin-Walled Structures, **49**(12), (2011), 1492–1503, DOI 10.1016/j.tws.2011.07.009.
- 7 **Gilbert BP, Savoyat TJ-M, Teh L**, *Self-shape optimisation application: Optimisation of cold-formed steel columns*, Thin-Walled Structures, **60**, (2012), 173–184, DOI 10.1016/j.tws.2012.06.008.
- 8 **Zeinoddini V, Schafer BW**, *Global imperfections and dimensional variations in cold-formed steel members*, International Journal of Structural Stability and Dynamics, **11**(05), (2011), 829–854, DOI 10.1142/S0219455411004361.
- 9 **Cheung YK**, *Finite strip method in structural analysis*, Pergamon Press, 1976.
- 10 **Schafer B, Ádány S**, *Buckling analysis of cold-formed steel members using CUFEM: Conventional and constrained finite strip methods*, In: **LaBoube RA, Yu W-W** (eds.), Proceedings of 18th International Specialty Conference on Cold-Formed Steel Structures; Orlando, Florida, USA, 2006.
- 11 **Visy D**, *Elastic and geometric stiffness matrices for the semi-analytical finite strip method*, In: **Józsa J, Lovas T, Németh R** (eds.), Proceedings of the Conference of Junior Researchers in Civil Engineering 2012; Budapest, Hungary, 2012.
- 12 **Ádány S, Joó A, Visy D**, *On the calculation of the critical moment to lateral-torsional buckling of beams: comparison of various methods*, In: **Topping BHV, Costa Neves LF, Barros RC** (eds.), The Twelfth International

- Conference on Civil, Structural and Environmental Engineering Computing; Funchal, Madeira, Portugal, 2009.
- 13 **Li Z, Schafer BW**, *Buckling analysis of cold-formed steel members with general boundary conditions using CUFSM: conventional and constrained finite strip methods*. In: **LaBoube RA, Yu W-W** (eds.), *Proceedings of the 20th International Specialty Conference on Cold-Formed Steel Structures*; St. Louis, Missouri, USA, 2010.
 - 14 *EN 1993-1-3:2006, Eurocode 3, Design of Steel Structures, Part 1-3: General rules, Supplementary rules for cold-formed thin gauge members and sheeting*.
 - 15 *CUFSM 4.05. Elastic buckling analysis of thin-walled members with general end boundary conditions*, <http://www.ce.jhu.edu/bschafer/cufsm>.
 - 16 *ANSYS Structural Mechanics, Release 13.0*, ANSYS, Inc.
 - 17 **Bebiano R, Pina P, Silvestre N, Camotim D**, *GBTUL – Buckling and Vibration Analysis of Thin-Walled Members*, DECivil/IST, Technical University of Lisbon, 2008, <http://www.civil.ist.utl.pt/gbt>.
 - 18 *North American Specification for the Design of Cold-Formed Steel Structural Members*, American Iron and Steel Institute, Washington, DC, USA, 2007.